JCTC Journal of Chemical Theory and Computation

Simulation of Actuation by Polymeric Polyelectrolyte Helicenes

Pawel Rempala and Benjamin T. King*

University of Nevada, Reno, Department of Chemistry/216, Reno, Nevada 89557

Received March 20, 2006

Abstract: The potential of several peripherally substituted [6.3.1] helicenes to serve as linear actuators was investigated using molecular dynamics calculations. Reversible extension upon ionization of pendant functionality was observed in three of four cases. The largest extensions were obtained for molecules with amino groups or ionized phosphate groups attached directly to the helical backbone (extensions of 176 ± 4% and 184 ± 4%, respectively). Electrostatic forces and swelling drive the actuation.

Introduction

Motion is a fundamental physical phenomenon. Indeed, the management and utilization of motion at the molecular level is an emerging theme in nanotechnology. Internal rotational motion in molecules and its potential use in molecular machines attracts considerable attention, as evidenced by a recent review article.[1] Interest in translational motion is also apparent, for example, research on rotaxanes as molecular shuttles.[2] Rotation may induce translation, as occurs in biological muscles. Of course, the cumulative function of molecular objects can produce macrosopic motion, as in artificial muscles.[3] Chemically driven artificial muscles have been demonstrated. For example, a film of triblock copolymer with hydrophobic ends [poly(methyl methacrylate)] and a midblock of poly(methacrylic acid) exhibited reversible actuation driven by changing pH.[4]

Biological molecular motors, which transform chemical energy into motion (e.g., the myosin−actin system[5]), are complex, and their synthetic imitation is daunting. We propose a synthetically feasible molecular actuator based on a springlike [6.3.1] helicene (we use Balaban's nomenclature[6] because IUPAC nomenclature is inadequate for this family of helicenes) with peripheral functionality (Figure 1). Ionization, as the result of a chemical reaction of peripheral functionality (Figure 2), could induce actuation.

The proposed systems possess the unusual combination of properties necessary for effective actuation: a high aspect ratio, elasticity, shape persistence, and the ability to change

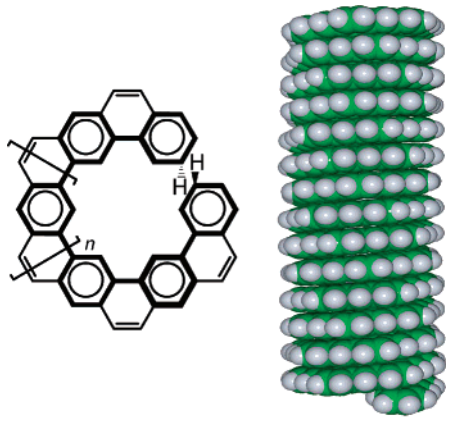

Figure 1. [6.3.1] helicene investigated as prospective actuator backbone.

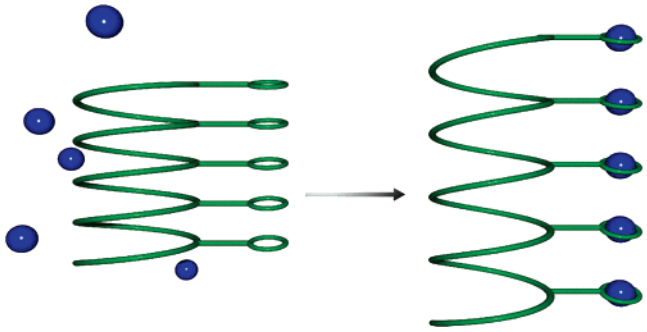

Figure 2. General concept of a chemically driven helical molecular actuator. Ions are represented by blue spheres.

chemical state. Most shape-persistent, high aspect ratio molecules, for example, poly(*p*-phenylene) and carbon nano-

* Corresponding author fax: (775) 784-6804; e-mail: king@chem.unr.edu.

10.1021/ct600102r CCC: $33.50 © 2006 American Chemical Society
Published on Web 06/21/2006

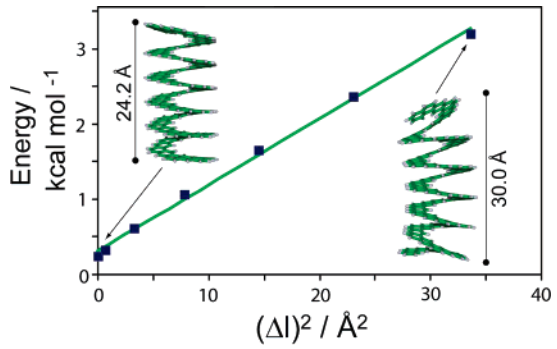

Figure 3. Energy of [6.3.1] helicene as a function of the square of extension from the equilibrium length.

tubes, are not easily stretched. Most polyelectrolytes and dopable polymers are not shape-persistent.

Elasticity, which is fundamental to actuation, is commonly expressed using Young's modulus (E). This intrinsic measure of elasticity is defined by eq 1, where A is the cross section area, l_0 is the unperturbed length, and l is the length when force F is applied.

$$E = Fl_0/A(l - l_0) = Fl_0/A\Delta l \quad (1)$$

We treat the helicene as a solid rod with a constant cross section. Energy as a function of length was obtained using the semiempirical PM3 Hamiltonian. For a spring obeying Hooke's law, the elastic potential energy, V, is described by eq 2, where k is the force constant. Hence, the total energy of the system (H_{tot}) should be a linear function of $(\Delta l)^2$, with a slope equal to $k/2$ (eq 3). Substituting $k\Delta l$ for F in eq 1 relates Young's modulus (E), the force constant, and the geometry (eq 4).

$$V = k(l - l_0)^2/2 = k(\Delta l)^2/2 \quad (2)$$

$$H_{tot} = H_0 + V = H_0 + k(\Delta l)^2/2 \quad (3)$$

$$E = (k\Delta l)l_0/A\Delta l = kl_0/A \quad (4)$$

Application of this protocol provided a Young's modulus of 0.16 GPa, compared to 7.5 GPa estimated for a conventional [6.2.1] helicene[7] (a [n]helicene in IUPAC nomenclature). To put these values into context, the Young's modulus of single-walled carbon nanotubes is ~1000 GPa,[8] steel is ~200 GPa, rubber is 0.01−0.1 GPa, and an α-helix peptide (poly-L-glutamic acid) is ~3 GPa.[9] The use of a single end-to-end distance constraint in these optimizations resulted in slightly bent geometries (Figure 3), but the expected linear relationship of energy versus $(\Delta l)^2$ held.

Our initial calculations in vacuo (PM3 and molecular mechanics) on charged helicenes indicated, not surprisingly, severalfold expansion as compared to that of neutral molecules. This vacuum treatment was unrealistic for many reasons. First, it was physically unreasonable—the real systems will operate in the condensed phase and will be electrically neutral. Second, if the system is treated as a set of collinear point charges fixed at even intervals, the electrostatic repulsion energy *per charge (monomer)* increases with the chain size without an upper bound. However, in the opposite limit, a disordered distribution of charge in an electroneutral system does not produce large potentials or fields.[10] For these reasons, the modeling of an intermediate case, in which charges are organized around a shape-persistent yet elastic backbone and counterions and a solvent are present, should be physically reasonable and could demonstrate actuation.

Methods

Molecular dynamics calculations were performed and analyzed using the Amber 7 suite of programs[11] (Leap, Sander, Carnal, and Antechamber[12]). The molecules studied are shown in Scheme 1 ($n = 31$). Both neutral and charged forms of the molecules were prepared in compact and extended conformations, and then atomic charges were assigned (see the Supporting Information for details). The charged forms were neutralized with Cl^- or K^+ ions during input preparation. Rectangular periodic boxes of TIP3P water[13] molecules were added next (approximately 5000−7000 water molecules). AMBER[14] and GAFF (General Amber Force Field)[15] force fields were applied to helicenes in the calculations. All calculations with TIP3P water were run at isobaric and isothermal conditions (target pressure of 1 bar, compressibility of water was assumed, target temperature 298 K) with a 1 fs integration step. To test whether swelling induced by the finite size of water molecules is important, some simulations were run using a generalized Born solvation model.[16,17] In this model, hydrophobic effects are represented using a surface energy term (gbsa=1 option, AMBER atom type). The screening effect of counterions was included by setting the monovalent salt concentration to 0.1 M (saltcon = 0.1, and also saltcon = 0.0 for comparison). Force field modifications, where a few missing torsional parameters were assumed to be identical to the available parameters based on chemical similarity, are given in the Supporting Information.

Results

All of the molecules investigated share a common backbone design. Their side chains were selected on the basis of synthetic accessibility and the ability to ionize (acid−base chemistry for molecules **A** and **B** and phosphorylation followed by deprotonation in the cases of **C** and **D**). In cases **A** and **B**, basic groups close to the backbone should result in a concentration of positive charge at the edge of the oligomer helix. In the oligoacid derived from the phosphorylation of oligophenol **C**, deprotonation will yield doubly charged negative groups, so even greater repulsion and expansion might be expected. System **D** has long and flexible *N*-acetylphosphoserine side chains, which further separate doubly charged phosphate groups from the backbone.

Phosphorylation, the first step in the biomimetic actuation mechanism of **C** and **D**, is ubiquitous in metabolism and is responsible for energy transformation and storage, enzymatic regulation, and signaling.[18] Kinases (phosphotransferases) catalyze the transfer of a phosphoryl group (terminal phosphoryl group of ATP) to acceptors such as hydroxyl, carboxy, or other phosphate groups.[18] Kinases capable of an indis-

Scheme 1. Potential Actuators Studied

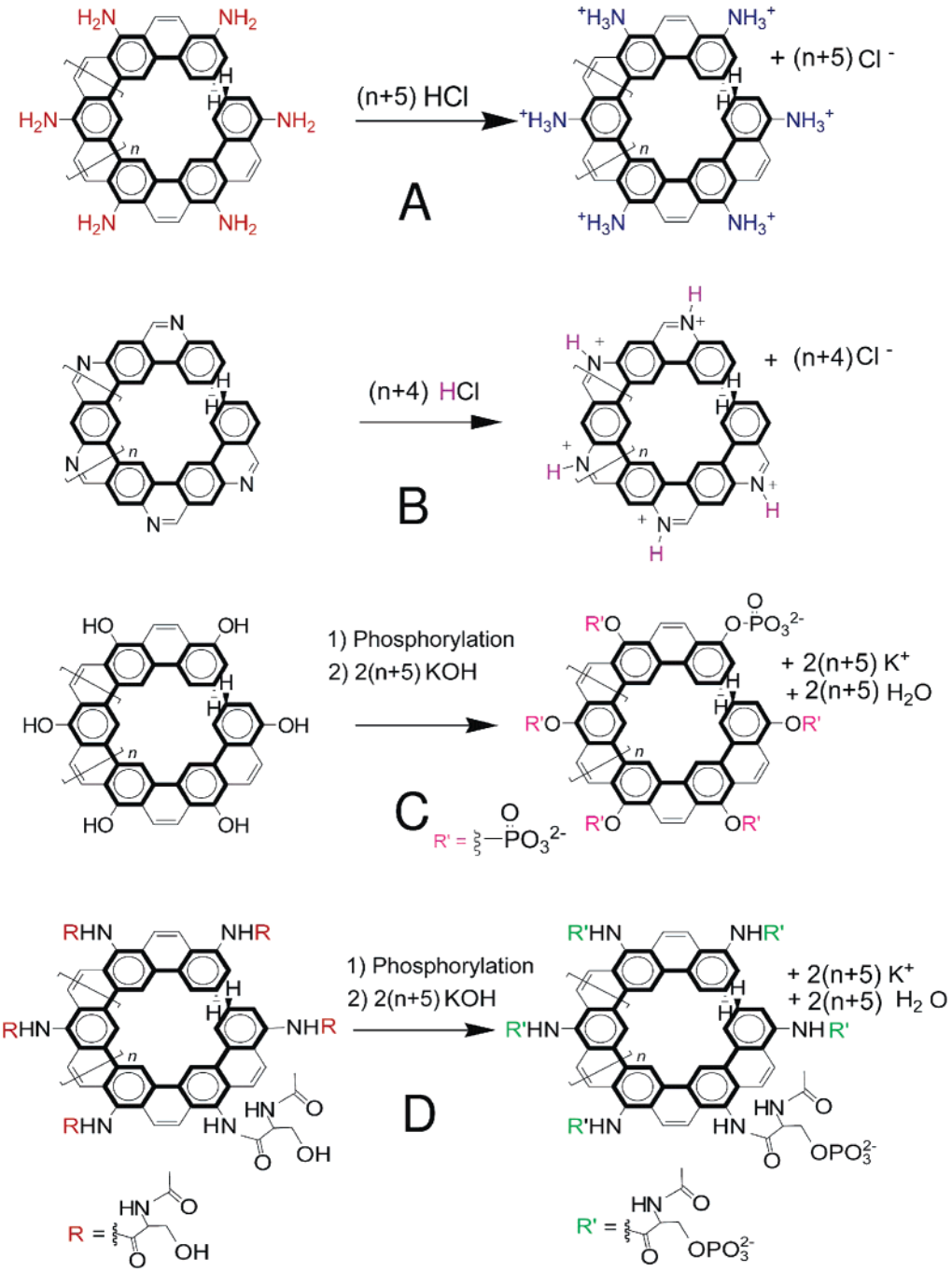

criminate phosphorylation of proteins are available.[19] Phosphorylation of the phenolic OH group in **C** and of the serine residues in **D** might be feasible under enzymatic catalysis, using ATP as a donor of the phosphate and an energy source.

The results for system **A** with explicit water are shown in Figure 4. Starting from a compact geometry, the neutral amino form of **A** remained compact over the time span of simulation (300 ps). Starting from a highly extended geometry, the neutral amino form of **A** contracts within 60 ps to the compact geometry. The attainment of the compact geometry from both compact and extended forms demonstrates that the equilibrium geometry of the neutral amino form of **A** is compact, with an end-to-end length of 20 Å. A similar set of calculations was performed on the protonated form of **A**. Starting from a compact geometry, the protonated form of **A** extends within 60 ps to an extended geometry. Starting from a highly extended geometry, the protonated form of **A** partially contracts within 60 ps to an extended geometry. This demonstrates that the equilibrium geometry of protonated **A** is extended, with an end-to-end length of 36 Å. The protonated form of **A** is (35.7 Å/20.3 Å) = 176% longer than the unprotonated form.

In the neutral molecule, favorable van der Waals attraction between hydrophobic hydrocarbon surfaces of the helix and minimization of the dihedral strain result in a compact structure. This compact structure, in which the tiers of atoms buttress one another, exhibits only small thermal variations in length. In the extended protonated form of **A**, which lacks the buttressing of the compact form, the end−end distance fluctuates somewhat.

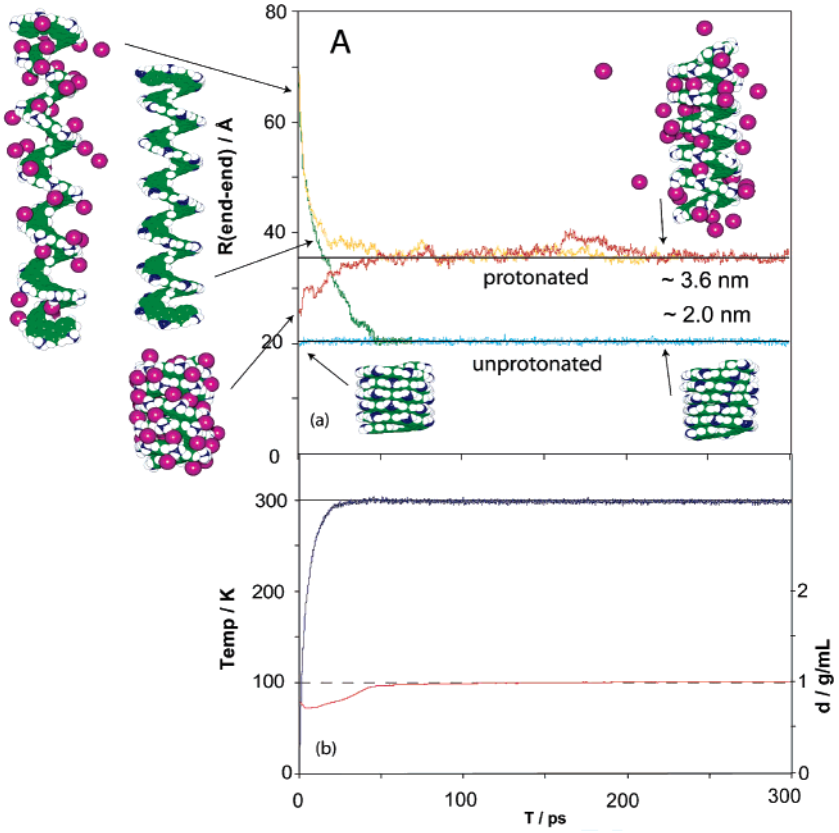

Figure 4. Summary of molecular dynamic simulation for system **A**, TIP3P water, periodic boundary conditions; chloride counterions are represented as purple spheres: (a) end−end distance as function of time and (b) evolution of temperature (blue) and density (red) for contraction of extended neutral form.

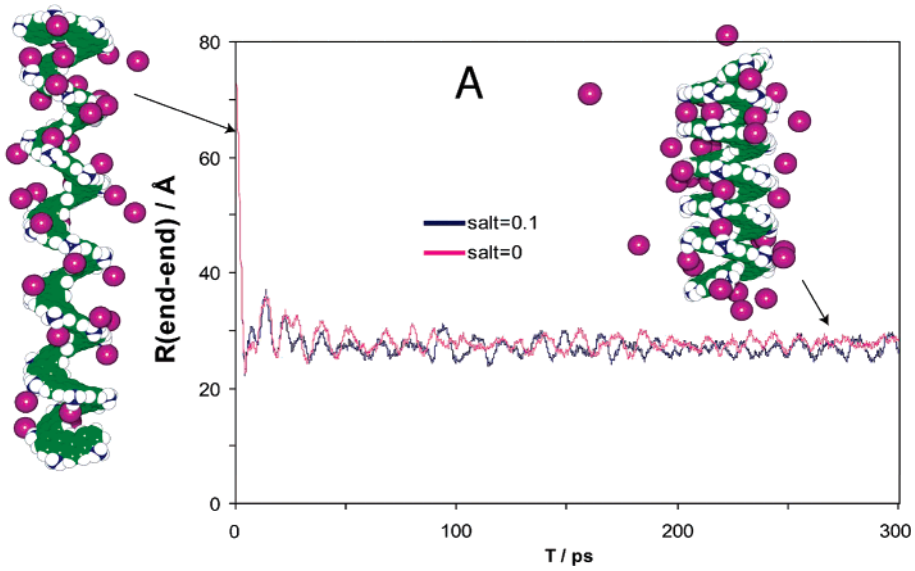

Figure 5. Results of molecular dynamic simulation for system **A** using a generalized Born solvation model. Chloride counterions are represented as purple spheres.

It is tempting to speculate, on the basis of trajectory snapshots, that the intercalation of chloride counterions stabilizes the extended geometry of protonated **A**. Inductive charge delocalization may also contribute to the extension by decreasing the hydrophobic forces on the helicene.

The chemical reactions that trigger actuation are not included in our simulations. The extended basic structure could arise from the rapid deprotonation of an extended oligo ammonium salt. Evidence exists that the inclusion of proton exchange dynamics can affect the molecular dynamic simulations of peptides.[20]

Two underlying mechanisms are responsible for the extension: electrostatic repulsion of the charged pendant groups and swelling induced by ions and their solvation. Simulations using a generalized Born solvation model, where the solvent was represented implicitly as a zero-viscosity

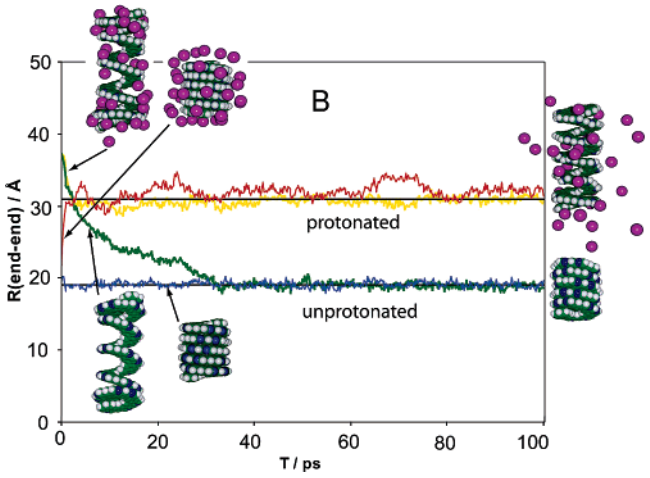

Figure 6. Summary of molecular dynamic simulation for system **B**. Chloride counterions are represented as purple spheres.

continuum with dielectric properties of water and an instantaneous dielectric response, revealed the relative contributions of these underlying phenomena. This model represents an aqueous electrolyte solution, but without the molecular bulk. If full extension occurs in this model, the mechanism of extension must be predominantly electrostatic repulsion, not swelling. If extension does not occur, the mechanism of extension is swelling. Two simulations (0 and 0.1 M salt concentrations) starting from the extended form of protonated **A** were performed. Chloride counterions provided electrical neutrality (Figure 5). The resulting equilibrium length (27.7 Å, 0.98 Å RMSD, 0 salt concentration, averaged over 100−300 ps interval) is between the equilibrium lengths of the simulation with explicit water molecules (35.7 Å) and those using the uncharged helicene (20.3 Å). Both mechanisms operate.

The comparison of the two solvation models requires addressing a few technical points. The generalized Born solvation model does not use periodic boundary conditions, which results in more accessible volume in the simulation. This permits the chloride ions to drift far from the helicene. For both 0 and 0.1 M salt solutions, the length oscillated on the ∼10 ps time scale, which is likely due to limited degrees of freedom in this rigid system lacking solvent molecules.

System **B** is similar to system to **A**, except that the basic nitrogen sites are incorporated into the backbone (i.e., pyridine versus aniline). The results are summarized in Figure 6.

The behavior of **B** is similar to that of **A**, with an actuation of 31.0 Å/19.0 Å = 163%. This system is also a viable synthetic target.

System **C** relies on a bioinspired two-stage actuation process. A parent helicene with pendant phenolic hydroxyl groups is phosphorylated, and then the resulting polyacid is deprotonated. The simulations were organized in the same manner as for systems **A** and **B**—approaching equilibrium from both directions for both the neutral and charged forms. The results are summarized in Figure 7. At equilibrium, actuator **C** exhibits similar behavior as actuator **A**—the neutral form is compact and the charged form is extended. Indeed, the extent of actuation, 37.1 Å/20.2 Å = 184%, is comparable.

The charged form of **C** shows greater variations in length than charged **A** and **B**. It is also important to note that this two-stage process, which increases molecular bulk [OP(O)-$(OH)_2$ vs OH] and charge (0 vs −2 per unit), does not increase the extension substantially.

System **D** is another bioinspired example which uses the same two-stage process, except, instead of simple hydroxyl groups, *N*-acetylserine side chains are used, which are more amenable to enzymatic phosphorylation. The simulations were performed as before: the equilibrium geometry of the charged and uncharged systems are approached from compact and extended forms. The results are summarized in Figure 8.

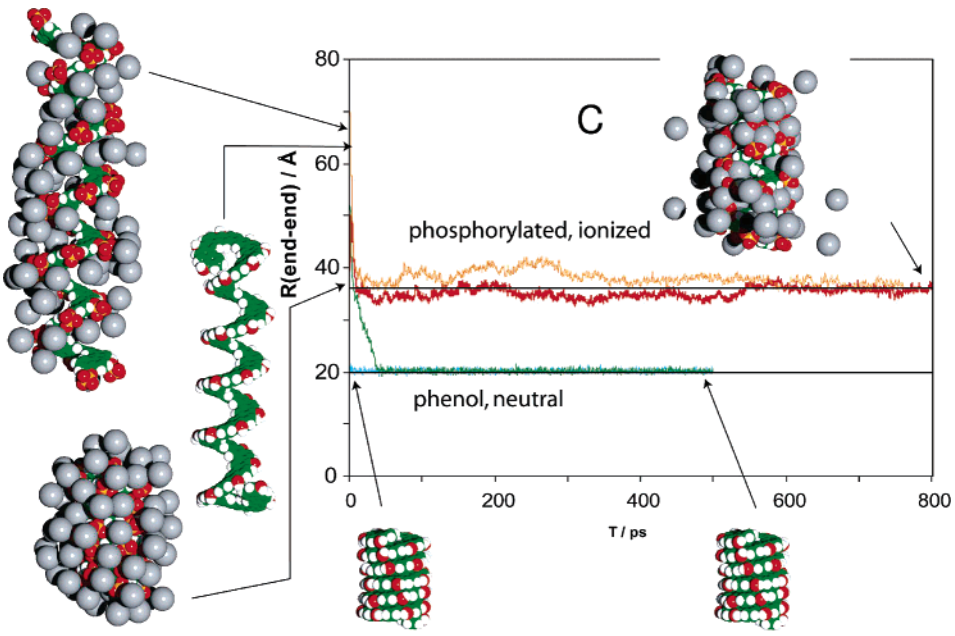

Figure 7. Summary of molecular dynamic simulation for system **C**. Potassium counterions are represented as grey spheres.

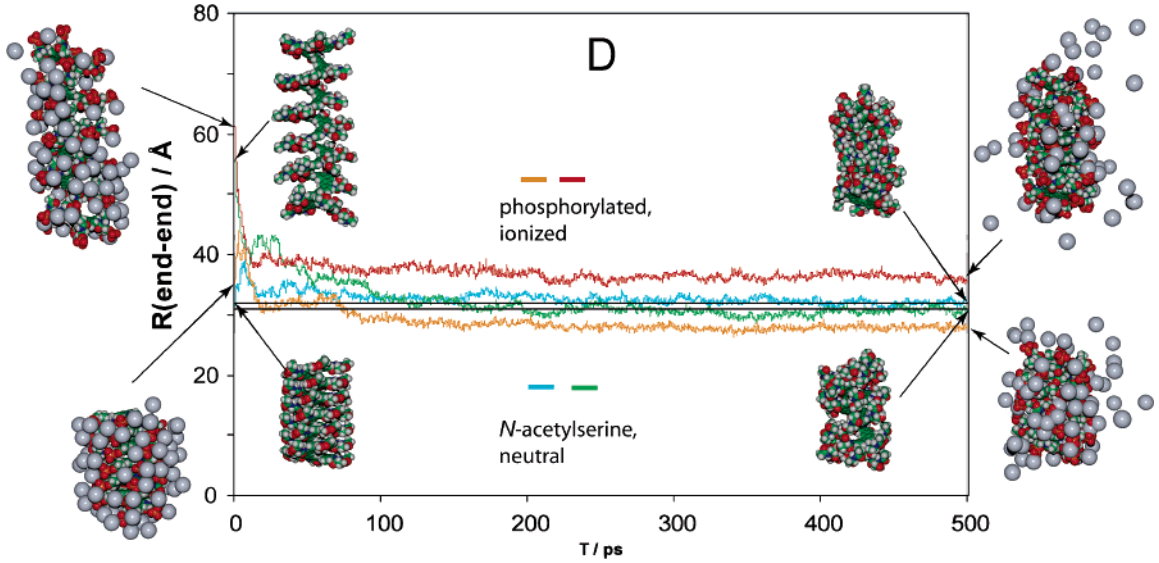

Figure 8. Summary of molecular dynamic simulation for system **D**.

Table 1. Results of MD Simulations for the Charged and Neutral Systems

system	neutral form end−end average/Å	RMSD/Å	charged form end−end average/Å	RMSD/Å	expansion, %	uncertainty,[e] %
A[a]	20.32	0.31	35.66	0.63	175.5	4.1
B[b]	18.98	0.35	31.03	0.50	163.5	4.0
C[c]	20.19	0.31	37.06	0.72	183.6	4.5
D[d]	31.27	1.03	32.05	4.31	102	14

[a] Neutral (base): average over 200−300 ps interval, compact starting geometry. Charged (hydrochloride): average over 200−300 ps, extended starting geometry. [b] Neutral (base): average over 200−300 ps interval, extended starting geometry. Charged (hydrochloride): average over 200−300 ps, extended starting geometry. [c] Neutral (phenol): average over 300−500 ps interval, extended starting geometry. Charged (phosphate potassium salt): average over 550−750 ps, extended starting geometry. [d] Neutral (amino acid): average over 300−500 ps for both trajectories (starting from compact and extended geometries) treated as one data population. Charged (phosphorylated, potassium salt) averaging same as for neutral. The trajectories in system **D** did not converge. [e] RMSDs for end−end distances treated as standard deviations to estimate uncertainty of length ratios.

System **D** does not exhibit actuation within 500 ps. Indeed, equilibrium is not achieved after 500 ps for both the charged and neutral forms, as the lengths depend on the initial geometry. In any case, actuation is not observed after 500 ps, whereas systems **A**, **B**, and **C** exhibit pronounced actuation within 60 ps. It is unlikely that system **D** could serve as a fast response actuator.

System **D** cannot actuate because it cannot contract—contraction is prevented by the steric bulk of the *N*-acetylserine tethers. Indeed, the equilibrium length of the neutral form of system **D** (31.3 Å) is similar to the equilibrium length of the charged forms of systems **A**, **B**, and **C** (35.7, 31.0, and 37.0 Å, respectively).

Conclusion

Our concept of a [6.3.1]-helicene-based, chemically driven molecular actuator seems viable on the basis of molecular dynamics calculations. A summary of results as ratios of lengths at the ionized and neutral states is given in Table 1. The steric bulk of the side chains reduces efficiency dramatically, and doubly charged groups do not improve efficiency compared to singly charged groups. The simple systems **A** and **B** and the biomimetic system **C** are good candidates for molecular actuators. Because the final states of the systems **A**, **B**, and **C** do not depend on the initial state, the actuation is reversible. Both electrostatic repulsion and swelling contribute to actuation.

Acknowledgment. We are grateful for generous support from the Department of Energy, the National Science Foundation (CHE- 0449740), the University of Nevada, and the Office of Naval Research.

Supporting Information Available: Trajectory animations for the contraction of uncharged system **A** and the extension of charged system **A**, details of modulus calculations, details of dynamics calculations, and modifications to the force field. This material is available free of charge via the Internet at http://pubs.acs.org.

References

(1) Kottas, G. S.; Clarke, L. I.; Horinek, D.; Michl, J. *Chem. Rev.* **2005**, *105*, 1281−1376.

(2) Jang, S. S.; Jang, Y. H.; Kim, Y.-H.; Goddard, W. A., III; Choi, J. W.; Heath, J. R.; Laursen, B. W.; Flood, A. H.; Stoddart, J. F.; Nørgaard, K.; Bjørnholm, T. *J. Am. Chem. Soc.* **2005**, *127*, 14804−14816.

(3) Lin, K.-J.; Fu, S.-J.; Cheng, C.-Y.; Chen, W.-H.; Kao, H.-M. *Angew. Chem., Int. Ed.* **2004**, *43*, 4186−4189.

(4) Howse, J. R.; Topham, P.; Crook, C. J.; Gleeson, A. J.; Bras, W.; Jones, R. A. L.; Ryan, A. J. *Nano Lett.* **2006**, *6*, 73−77.

(5) Piazzesi, G.; Reconditi, M.; Linari, M.; Lucii, L.; Sun, Y.-B.; Narayanan, T.; Boesecke, P.; Lombardi, V.; Irving, M. *Nature* **2002**, *415*, 659−662.

(6) Balaban, A. T. *Polycyclic Aromat. Compd.* **2003**, *23*, 277−296.

(7) Jalaie, M.; Weatherhead, S.; Lipkowitz, K. B.; Robertson, D. *Electron. J. Theor. Chem.* **1997**, *2*, 268−272.

(8) Salvetat, J.-P.; Briggs, G. A. D.; Bonard, J.-M.; Bacsa, R. R.; Kulik, A. J.; Stöckli, T.; Burnham, N. A.; Forró, L. *Phys. Rev. Lett.* **1999**, *82*, 944−947.

(9) Idiris, A.; Alam, M. T.; Ikai, A. *Protein Eng., Des. Sel.* **2000**, *13*, 763−770.

(10) Singer, A.; Schuss, Z.; Eisenberg, R. S. *J. Stat. Phys.* **2005**, *119*, 1397−1418.

(11) Case, D. A.; Pearlman, D. A.; Caldwell, J. W.; Cheatham, T. E., III; Wang, J.; Ross, W. S.; Simmerling, C.; Darden, T.; Merz, K. M.; Stanton, R. V.; Cheng, A.; Vincent, J. J.; Crowley, M.; Tsui, V.; Gohlke, H.; Radmer, R.; Duan, Y.; Pitera, J.; Massova, I.; Seibel, G. L.; Singh, U. C.; Weiner, P.; Kollman, P. A. *Amber 7*; University of California: San Francisco, CA, 2002.

(12) Wang, J.; Wang, W.; Kollman, P. A.; Case, D. A. *J. Mol. Graphics Modell.* **2006**, in press. http://amber.scripps.edu/antechamber/antechamber.html (accessed September 8, 2004).

(13) Jorgensen, W. L.; Chandrasekhar, J.; Madura, J. D. *J. Chem. Phys.* **1983**, *79*, 926−935.

(14) Cornell, W. D.; Cieplak, P.; Bayly, C. I.; Gould, I. R.; Merz, K. M., Jr.; Ferguson, D. M.; Spellmeyer, D. C.; Fox, T.; Caldwell, J. W.; Kollman, P. A. *J. Am. Chem. Soc.* **1995**, *117*, 5179−5197.

(15) Wang, J.; Wolf, R. M.; Caldwell, J. W.; Kollman, P. A.; Case, D. A. *J. Comput. Chem.* **2004**, *25*, 1157−1174.

(16) Hawkins, G. D.; Cramer, C. J.; Truhlar, D. G. *Chem. Phys. Lett.* **1995**, *246*, 122−129

(17) Hawkins, G. D.; Cramer, C. J.; Truhlar, D. G. *J. Phys. Chem.* **1996**, *100*, 19824−19839.

(18) Horton, H. R.; Moran, L. A.; Ochs, R. S.; Rawn, J. D.; Scrimgeour, K. G. *Principles of Biochemistry*, 2nd ed.; Prentice Hall: Upper Saddle River, NJ, 1996.

(19) Hubbard, S. R.; Till, J. H. *Annu. Rev. Biochem.* **2000**, *69*, 373−398.

(20) Długosz, M.; Antosiewicz, J. M. *J. Phys. Chem. B* **2005**, *109*, 13777−13784.

CT600102R